

pubs.acs.org/est Article

# Real-Time Measurements of Gas-Phase Trichloramine (NCl<sub>3</sub>) in an Indoor Aquatic Center

Tianren Wu, Tomas Földes, Lester T. Lee, Danielle N. Wagner, Jinglin Jiang, Antonios Tasoglou, Brandon E. Boor,\* and Ernest R. Blatchley III\*



Cite This: Environ. Sci. Technol. 2021, 55, 8097-8107



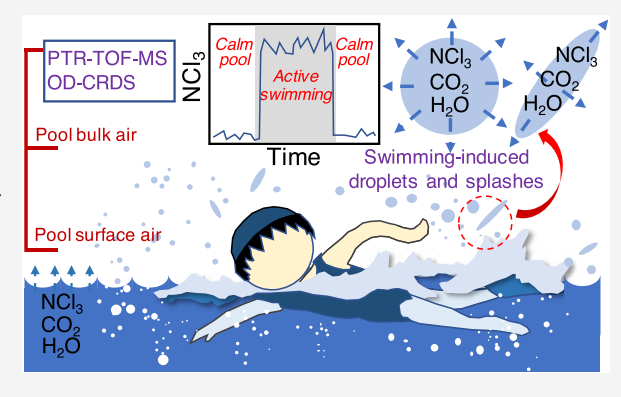
**ACCESS** 

Metrics & More

Article Recommendations

Supporting Information

ABSTRACT: NCl<sub>3</sub> is formed as a disinfection byproduct in chlorinated swimming pools and can partition between the liquid and gas phases. Exposure to gas-phase NCl<sub>3</sub> has been linked to asthma and can irritate the eyes and respiratory airways, thereby affecting the health and athletic performance of swimmers. This study involved an investigation of the spatiotemporal dynamics of gas-phase NCl<sub>3</sub> in an aquatic center during a collegiate swim meet. Real-time (up to 1 Hz) measurements of gas-phase NCl<sub>3</sub> were made via a novel on-line derivatization cavity ring-down spectrometer and a proton transfer reaction time-of-flight mass spectrometer. Significant temporal variations in gas-phase NCl<sub>3</sub> and CO<sub>2</sub> concentrations were observed across varying time scales, from seconds to hours. Gas-phase NCl<sub>3</sub> concentrations increased with the number of active swimmers due to swimming-enhanced liquid-to-gas



transfer of NCl<sub>3</sub>, with peak concentrations between 116 and 226 ppb. Strong correlations between concentrations of gas-phase NCl<sub>3</sub> with concentrations of CO<sub>2</sub> and water (relative humidity) were found and attributed to similar features in their physical transport processes in pool air. A vertical gradient in gas-phase NCl<sub>3</sub> concentrations was periodically observed above the water surface, demonstrating that swimmers can be exposed to elevated levels of NCl<sub>3</sub> beyond those measured in the bulk air.

KEYWORDS: indoor air quality, swimming pool chemistry, volatile disinfection byproducts, cavity ring-down spectroscopy, proton transfer reaction time-of-flight mass spectrometry

# INTRODUCTION

Swimming is the second most common form of exercise in the United States. The majority of swimming activity takes place in controlled settings (e.g., swimming pools) in which an essentially fixed volume of water is used, often with minimal replacement, over periods of several months. This requires continuous water treatment, including the application of one or more disinfection processes to control exposure to microbial pathogens. The default method of disinfection is addition of chlorine, which also oxidizes organic and inorganic contaminants that are introduced to pool water by swimmers. However, the reactivity of +1-valent chlorine results in the formation of a wide range of disinfection byproducts (DBPs), some of which are known to be associated with adverse human health effects. Among the DBPs formed in pools are roughly 10 volatile compounds<sup>2-8</sup> By definition, these compounds have the ability to partition between the liquid and gas phases. As such, volatile DBPs in swimming pools are known to contribute to the degradation of indoor air quality (IAQ) in indoor swimming pool facilities.

Among the volatile DBPs that are formed in chlorinated pools, trichloramine (NCl<sub>3</sub>) is particularly noteworthy. <sup>9–12</sup> NCl<sub>3</sub> is largely responsible for the characteristic "chlorine"

odor that is often associated with chlorinated indoor pools. As a volatile form of +1-valent chlorine, NCl<sub>3</sub> functions as an irritant to the upper respiratory system, has been linked to respiratory ailments such as asthma, <sup>13-19</sup> and is suspected to contribute to corrosion of metallic surfaces in swimming pool facilities, including heating, ventilation, and air conditioning (HVAC) system components. <sup>20</sup> NCl<sub>3</sub> is formed as a result of reactions between +1-valent chlorine and a wide range of organic-N compounds that are introduced to pools largely through excretion of urine and sweat. <sup>8</sup> Known precursors to NCl<sub>3</sub> formation include urea, uric acid, creatinine, and amino acids. <sup>8</sup> The concentration of NCl<sub>3</sub> in pool water can also be affected by other forms of treatment, notably by the inclusion of UV-based treatment. UV irradiation of pool water will generally result in decreases in the concentration of inorganic chloramines, <sup>21</sup> including NCl<sub>3</sub>, via photolysis. <sup>21-23</sup> However, it

Received: November 3, 2020 Revised: April 21, 2021 Accepted: April 22, 2021 Published: May 25, 2021





should be recognized that UV irradiation can initiate competing reactions that will actually promote  $NCl_3$  formation.  $^{24-26}$ 

Previous research has demonstrated that the transfer of NCl<sub>3</sub> from the liquid phase to the gas phase is promoted by the mixing energy imparted to water by swimmers.<sup>7,11</sup> This observation is consistent with two-film theory of interphase transport,<sup>27</sup> and suggests that the processes that promote the net transfer of NCl<sub>3</sub> from the liquid phase to the gas phase are also likely to promote the net transfer of other volatile compounds that are commonly observed in swimming pool water and that have Henry's law constants that are similar to that of NCl<sub>3</sub>. As such, NCl<sub>3</sub> serves as a sentinel compound for IAQ in indoor swimming pool facilities.

To date, only a limited number of studies have been conducted to define the dynamics of gas-phase NCl<sub>3</sub> in indoor swimming pool facilities. Most published work has involved analytical methods that are able to provide meaningful measurements of the gas-phase NCl<sub>3</sub> concentration at a time increment of 30–60 min or longer. Given the nature of human exposure to indoor air in these facilities, there is a need to understand these dynamics at a finer time scale.

The dynamic behavior of gas-phase NCl<sub>3</sub> in indoor swimming facilities is related to its rate of formation in the liquid phase, the number of swimmers in the facility and the nature of their activities, the presence or absence of "spray features," as well as the design and operational characteristics of HVAC systems that are used to control air circulation and air quality. <sup>11,28,31</sup> At present, these dynamics are only understood in a qualitative sense. A need exists to develop quantitative design guidelines for indoor pools to promote improvements in IAQ. These guidelines will depend on a detailed, quantitative understanding of the processes that govern IAQ dynamics, particularly, as related to NCl<sub>3</sub>.

In recent years, advanced analytical techniques commonly used in atmospheric chemistry research for real-time monitoring of organic and inorganic gases have been applied to the study of indoor air. 32-38 This has generated new insights into the transport and transformation of indoor gaseous pollutants. To advance knowledge on dynamic inhalation exposures to NCl<sub>3</sub> in indoor swimming pools, we deployed novel analytical instruments with a multilocation sampling system to characterize spatiotemporal trends in gas-phase NCl<sub>3</sub> in an indoor aquatic center during a collegiate swim meet. Gasphase NCl<sub>3</sub> was continuously monitored with a time resolution up to 1 Hz using a proton transfer reaction time-of-flight mass spectrometer (PTR-TOF-MS) with both  $H_3O^+$  and  $O_2^+$  as the reagent ions, an on-line derivatization cavity ring-down spectrometer (OD-CRDS), and two next environmental monitoring (NEMo) IAQ monitors. The OD-CRDS measures an absolute concentration of gas-phase NCl3. Gas-phase carbon dioxide (CO<sub>2</sub>) was measured as it could potentially be used to predict NCl3 concentrations and the number of active swimmers in a pool.<sup>31</sup> The impact of active swimmers on gas-phase NCl3 concentrations was investigated and the field performance of the three measurement techniques was compared. The concurrent measurement of NCl3 and complementary parameters, including gas-phase CO2, relative humidity (RH), and swimmer counts, provides a basis for new insights into the liquid-to-air transport process of NCl<sub>3</sub>.

## MATERIALS AND METHODS

**Study Site: Indoor Aquatic Center.** Measurements were conducted at an indoor aquatic center during an invitational collegiate swim meet held from November 21 to 24, 2019. Roughly 350 swimmers from several universities participated in the meet. Additional details are provided in the Supporting Information (SI).

Liquid-Phase Measurements of Volatile DBPs. Pool water samples were collected from 30 cm below the water surface at a fixed location in the pool. The samples were immediately subjected to analysis using a portable membrane introduction mass spectrometry (MIMS) system (HPR-40 DSA, Hiden Analytical, Warrington, United Kingdom), which was installed in an office adjacent to the pool deck. Liquid-phase concentrations of NCl<sub>3</sub> were quantified based on comparison of m/z abundance signals with standard curves that had been developed prior to the experiment. The detection limit was 0.1 mg L<sup>-1</sup>. For the water samples collected during this experiment, NCl<sub>3</sub> was present at concentrations that were consistently below the detection limit for this instrument.

Gas-Phase NCl<sub>3</sub> Measurements. The gas-phase concentration of NCl<sub>3</sub> was monitored using a PTR-TOF-MS (PTR-TOF 4000, Ionicon Analytik GmbH, Innsbruck, Austria), an OD-CRDS (built-in-house), and two NEMo IAQ monitors (Ethera Labs, Crolles, France). The OD-CRDS provides the absolute measurement of gas-phase NCl<sub>3</sub>. The inlets of the PTR-TOF-MS and OD-CRDS were connected to an automated switching valve system to sample among four sampling locations (Figure S1). One of the NEMo monitors (NEMo A) was mounted on the wall at a height ~4.7 m above the pool surface. Another NEMo monitor (NEMo B) was mounted on the lifeguard chair at a height ~1.2 m above the pool surface.

The OD-CRDS is a new absolute and real-time NCl<sub>3</sub> measurement technique developed at the Université libre de Bruxelles (ULB). In this approach, NCl<sub>3</sub> is on-line derivatized to NH<sub>3</sub> and the NCl<sub>3</sub> concentration is determined by measuring the generated NH<sub>3</sub> concentration by a continuous-wave CRDS. A filter containing solid Na<sub>2</sub>SO<sub>3</sub> powder was used for the derivatization. The probable reaction scheme is the same as the one demonstrated in the liquid phase, <sup>39,40</sup> with a stepwise nature. NCl<sub>3</sub> and Na<sub>2</sub>SO<sub>3</sub> react to eventually form NH<sub>3</sub> with intermediate formation of NHCl<sub>2</sub>, NH<sub>2</sub>Cl, and ClSO<sub>3</sub><sup>-</sup>, e.g., <sup>40</sup>

$$NCl_3 + SO_3^{2-} + H_2O \rightarrow NHCl_2 + ClSO_3^{-} + OH^{-}$$
(1)

$$NHCl_2 + SO_3^{2-} + H_2O \rightarrow NH_2Cl + ClSO_3^{-} + OH^{-}$$
(2)

The  $NH_2Cl$  to  $NH_3$  reaction is general-acid (HA) assisted  $^{40}$ 

$$HA + NH_2Cl + SO_3^{2-} \rightarrow A^- + NH_3 + ClSO_3^-$$
 (3)

A citric or sulfamic acid prefilter was used upstream of the sulfite filter to trap  $NH_3$  in the sampled air, similar to acid-coated denuders or acid-impregnated filters for ambient  $NH_3$  and ammonium collection. Advantageously, the same filter also removes  $NH_2Cl$  and  $NHCl_2$  from the airstream in a manner similar to the silica gel-sulfamic acid filter used in the "Hery method" commonly used for offline  $NCl_3$  measurement. Since the stoichiometry of the  $NCl_3$  to  $NH_3$  reaction is 1:1, the determined  $NH_3$  concentrations correspond to the

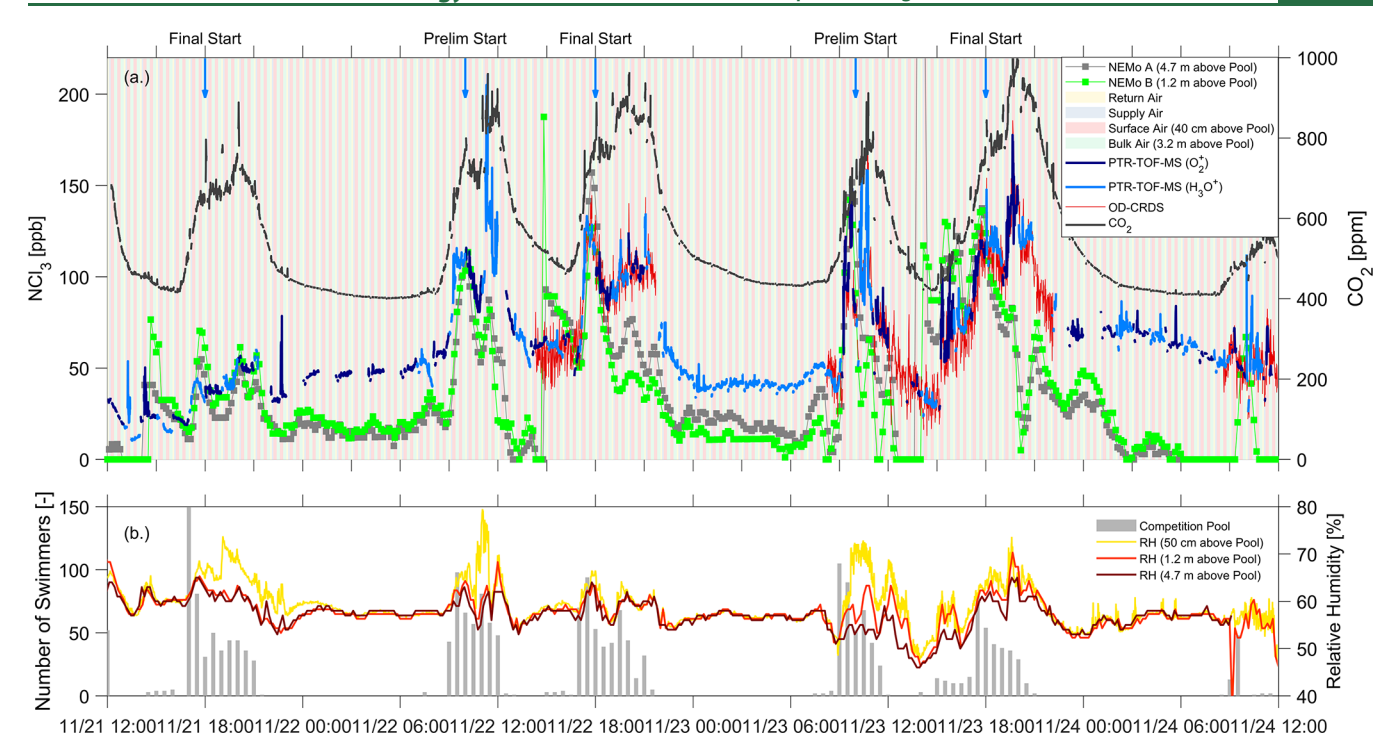


Figure 1. (a) Time-series plot of the spatially resolved gas-phase NCl<sub>3</sub> concentration measured by the PTR-TOF-MS (dark and light blue line) and OD-CRDS (red line), and CO<sub>2</sub> concentration (dark gray line) over the entire measurement campaign. The color-coded background indicates the sampling locations (including return air, supply air, pool surface air, and pool bulk air) for a given period. The NCl<sub>3</sub> concentration was also measured by two stationary NEMo monitors at heights of 4.7 and 1.2 m above the pool surface. The NCl<sub>3</sub> concentration measured by the PTR-TOF-MS and the CO<sub>2</sub> concentration are shown as a 30 s average. (b) Time-series plot of swimmer counts in the competition pool (gray bars; the left axis) and relative humidity (yellow, orange, and dark red lines; the first right axis). Relative humidity was recorded by the Lascar temperature and humidity logger (yellow line) at a height 50 cm above the pool surface and two NEMo monitors at heights of 1.2 m (orange line) and 4.7 m (dark red line) above the pool surface.

NCl<sub>3</sub> concentrations upstream of the sulfite filter. The OD-CRDS approach has been validated in several intercomparison studies (not yet published) with the Hery method<sup>44</sup> and adapted Hery method with colorimetric analysis (Triklorame kit, Syclope Electronique, France). An example is shown in the SI (Figure S17).

The operating principle of the CRDS is the same as first described by Romanini and co-workers. The design has been inspired by some previous instruments. It was configured to complete a full measurement loop in 2 min during the campaign. In each loop, the NCl<sub>3</sub> concentration was determined two times. Details of the design and configuration of the CRDS can be found in the SI. OD-CRDS measurements were conducted from 2 PM on November 22 until the end of the swim meet, but only during the pool opening hours. The NEMo device is a passive IAQ monitor that can be configured to measure gas-phase NCl<sub>3</sub>; <sup>49,50</sup> details on the governing measurement technique are provided in the SI.

The PTR-TOF-MS measured gas-phase  $NCl_3$  at a rate of 1 Hz. It switched between two primary reagent ions,  $H_3O^+$  and  $O_2^+,^{51}$  every hour. Under the  $H_3O^+$  mode,  $NCl_3$  is ionized via the proton-transfer reaction with  $H_3O^+$  as the proton affinity of  $NCl_3$  (721.5 kJ mol<sup>-1</sup>)<sup>52</sup> is greater than water (691 kJ mol<sup>-1</sup>). Under the  $O_2^+$  mode, the ionization of  $NCl_3$  occurs in a drift tube via a charge-transfer reaction with  $O_2^+,^{51,53}$  The abundance of impurity ions was less than 5% under both modes. The measurements with the PTR-TOF-MS started at 12 PM on November 21 and lasted until the end of the swim meet. Calibration and operational conditions are described in the SI.

Due to the lack of a calibration standard for NCl<sub>3</sub>, we corrected the NCl<sub>3</sub> concentration measured with the PTR-TOF-MS in each mode against the absolute measurement with the colocated OD-CRDS. This correction was done daily. First, the signals of product ions of the proton or charge-transfer reactions were adjusted for ion transmission and the isotopic signals were combined. The product ions used for concentration calculation under the H<sub>3</sub>O<sup>+</sup> mode include NCl<sub>3</sub>H<sup>+</sup> and an identified fragment  $NCl_2^+$  ( $R^2 = 0.99$ , Figure S2). The product ions under the  $O_2^+$  mode include  $NCl_3^+$  and the fragment  $NCl_2^+$  ( $R^2 = 0.99$ , Figure S3), which has been reported in previous measurements with selected ion flow tube-mass spectrometry (SIFT-MS) with O2+ serving as the reagent ion. 53,54 The signals of the product ions were then converted to the theoretical concentration under each mode, assuming a default reaction rate coefficient of  $2 \times 10^{-9}$  cm<sup>3</sup> s<sup>-1</sup>.55 Following this, the theoretical concentrations for each day were scaled by a correction factor, which was obtained via linear regression between the theoretical concentrations and the absolute concentrations measured by the OD-CRDS. The uncertainties of the corrected concentrations were ±11.11 and  $\pm 12.33\%$  under the  $O_2^+$  and  $H_3O^+$  modes (Figures S4 and S5), respectively, obtained as the mean absolute percentage error between the corrected concentration and the concentration measured by the OD-CRDS from November 22 to 24. Additional details regarding the correction of the concentrations measured by the PTR-TOF-MS are included in the SI.

Additional Measurements. Gas-phase CO<sub>2</sub> concentrations were monitored using a CO<sub>2</sub> gas analyzer (LI-830, LI-COR Biosciences, Lincoln, Nebraska, U.S.A.). It was calibrated

by the manufacturer in early 2019. The inlet of the CO<sub>2</sub> gas analyzer was also connected to the automated switching valve system as described above for the PTR-TOF-MS and OD-CRDS. RH was monitored 0.5 m above the pool surface, close to the pool surface, and at the bulk air sample inlets of the automated valve system, by a temperature and RH logger (EL-USB-2-LCD, Lascar Electronics Ltd., Wiltshire, United Kingdom). RH was also recorded by the NEMo monitors. The number of swimmers in the competition pool and other locations throughout the aquatic center were counted throughout the swim meet every 30 min. A preliminary pilot campaign was conducted at the aquatic center from September 25 to 28, 2019; selected results are shown in Figure S9.

Automated Valve System for Spatially Resolved Indoor Air Sampling. An automated valve system allowed for periodic sampling at different locations to investigate the spatial variation of gas-phase NCl<sub>3</sub> and CO<sub>2</sub> concentrations. Four sampling locations included: one of the return air grilles (return air), one of the supply air ducts (supply air), 40 cm above the pool surface (pool surface air), and 3.2 m above the pool surface (pool bulk air) (Figure S1). The sampling sequence was repeated as follows: return air (6 min), surface air (12 min), surface air (12 min), with a full cycle of 60 min. Additional details are provided in the SI.

## ■ RESULTS AND DISCUSSION

The following terms: NCl<sub>3[PTR-MS]</sub>, NCl<sub>3[OD-CRDS]</sub>, NCl<sub>3[NEMo A]</sub>, and NCl<sub>3[NEMo B]</sub> are used to represent NCl<sub>3</sub> concentrations measured by the PTR-TOF-MS, OD-CRDS, NEMo A (4.7 m above pool surface), and NEMo B (1.2 m above pool surface), respectively, all of which are expressed as volume mixing ratios (in ppb).

Hourly and Daily Temporal Variations in Gas-Phase NCl<sub>3</sub> Concentrations During the Swim Meet. The timeand location-resolved gas-phase NCl<sub>3</sub> and CO<sub>2</sub> concentrations over the entire swim meet are shown in Figure 1a, with the color-coded background indicating the different sampling locations for the OD-CRDS, PTR-TOF-MS, and CO2 gas analyzer. Figure 1b shows the corresponding swimmer counts in the competition pool and RH measured at three different locations. Changes in the number of swimmers and ventilation conditions drove significant temporal variations in the gasphase NCl<sub>3</sub> concentration in the aquatic center. Over the entire measurement period, NCl<sub>3[PTR-MS]</sub> and NCl<sub>3[OD-CRDS]</sub> ranged from 22 to 114 and 30 to 123 ppb (5th-95th percentiles) in the pool bulk air, with mean concentrations of 67 and 75 ppb, respectively. The NCl<sub>3[NEMo A]</sub> and NCl<sub>3[NEMo B]</sub> ranged from 0 to 108 and 0 to 107 ppb (5th-95th percentiles), with mean concentrations of 37 and 38 ppb, respectively.

NCl<sub>3</sub> concentrations increased dramatically during active periods of swimming. Four peaks in the NCl<sub>3</sub> concentration profile can be clearly observed in the morning and evening on November 22 and 23, corresponding to the periods of the preliminary and final races of the swim meet. Immediate increases in the NCl<sub>3</sub> concentrations were observed at ~9 AM and ~5 PM on November 22 and 23, corresponding with increases in the number of swimmers in the pool during warm up and competition periods. The concentration remained elevated with consistently high swimmer counts during the sessions. A decay in gas-phase NCl<sub>3</sub> concentrations was observed at around 12 PM and 10 PM on November 22 and

23, corresponding to notable decreases in the number of swimmers. The peak concentrations of  $NCl_{3[PTR-MS]}$  and  $NCl_{3[OD-CRDS]}$  over these four periods were between 116 and 226 and 133 and 155 ppb, and the mean concentrations were 100 and 102 ppb in the bulk air, respectively, with mean swimmer counts of 52. The strong correlation between gasphase  $NCl_3$  concentrations and bather load has been reported in previous studies,  $^{11,13,28}$  and it has been attributed to the intense mixing of pool water due to the increased number of swimmers, which leads to enhanced liquid-to-gas transfer of  $NCl_3$ . According to Schmalz et al.  $^{30}$  the mass-transfer coefficient of  $NCl_3$  can increase from  $1.8 \times 10^{-3}$  g h $^{-1}$  m $^{-2}$  in a quiescent pool to  $7.0 \times 10^{-3}$  g h $^{-1}$  m $^{-2}$  by swimming activity and even to  $12.6 \times 10^{-3}$  g h $^{-1}$  m $^{-2}$  by increased splashing activity.

The increase in the number of swimmers can increase the aqueous-phase concentration of  $NCl_3$  precursors. This could result in a higher  $NCl_3$  concentration in the aqueous phase, causing a substantial increase in the gas-phase concentration. However, the associated water chemistry occurs over long time scales and is unlikely to cause an immediate jump in the gas-phase  $NCl_3$  concentration following a sudden increase in swimmers. Pool water was analyzed for  $NCl_3$  content; however, the aqueous-phase concentrations remained below the limit of detection of the analytical technique.

Mass transfer of NCl<sub>3</sub> from the liquid phase to the gas phase is also influenced by environmental factors, including temperature and pH. Temperature affects the escaping potential for volatile DBPs, as indicated by the effect of temperature on Henry's law constants of these compounds. In general, Henry's law constants display temperature dependence that can be described by the Van't Hoff equation.<sup>57</sup> Solution pH may also be relevant as it influences the distribution of the inorganic chloramines.<sup>58,59</sup>

The gas-phase  $\mathrm{CO}_2$  concentration increased with swimmer counts, following a similar trend as that of the gas-phase  $\mathrm{NCl}_3$  concentration. Sudden rises and gradual decays in gas-phase  $\mathrm{CO}_2$  concentrations were observed at the beginning and end of the preliminary and final races on November 22 and 23, with peak concentrations between 903 and 922 ppm in the bulk air during the sessions. Even though the audience and the swimmers can emit  $\mathrm{CO}_2$  via exhaled breath, the enhanced liquid-to-gas transfer caused by the intense, swimming-induced mixing of pool water also contributed significantly to the elevated gas-phase  $\mathrm{CO}_2$  concentration.  $\mathrm{CO}_2$  is added to pool water via the water treatment system at the aquatic center prior to the addition of  $\mathrm{Ca}(\mathrm{OCl})_2$  disinfectant.  $\mathrm{CO}_2$  addition is used for pH control.  $\mathrm{^{60,61}}$ 

Two-film theory suggests that the transfer of compounds from the liquid to gas phase is strongly influenced by their respective Henry's law constants (H).<sup>27</sup> Specifically, for compounds with large values of H, resistance to transport is governed by "liquid-film resistance." By extension, this explanation of liquid-to-gas transfer implies that the physical conditions that are responsible for the transfer of a compound with a relatively large value of H will also cause the transfer of other compounds that have similar values of H. NCl<sub>3</sub> and CO<sub>2</sub> are both relatively volatile, with Henry's law constants that are within a factor of two of each other (see Table S1 in the SI). As such, it is reasonable to expect that their respective potentials for the net transfer from the liquid phase to the gas phase would be similar. In turn, this would lead to similar patterns in

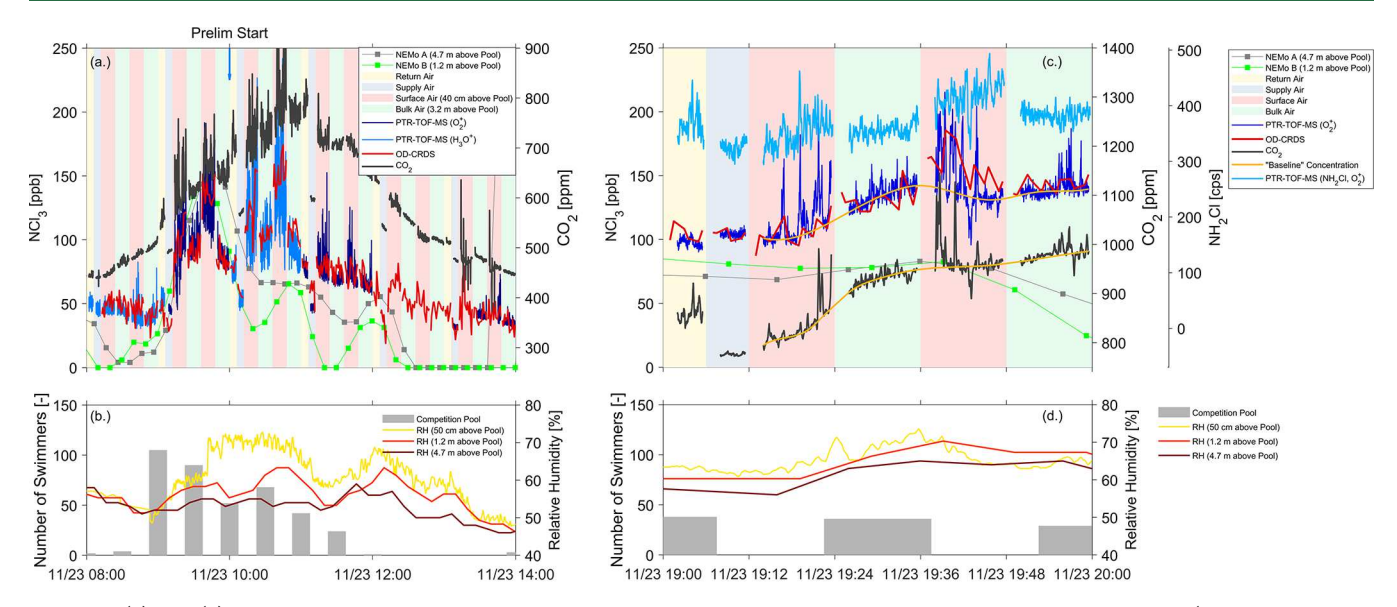


Figure 2. (a) and (c) Time-series plot of the spatially resolved gas-phase NCl<sub>3</sub> concentration measured by the PTR-TOF-MS (dark and light blue lines) and OD-CRDS (red line), and CO<sub>2</sub> concentration (dark gray line) over two active periods of swimming. The color-coded background indicates the sampling locations (including return air, supply air, pool surface air, and pool bulk air) for a given period. The NCl<sub>3</sub> concentration was also measured by two stationary NEMo monitors at heights of 4.7 and 1.2 m above the pool surface. The time resolution of the NCl<sub>3</sub> concentration measured by the PTR-TOF-MS and the CO<sub>2</sub> concentration is 1 s. The light blue line in (c) represents the counts per second (cps) of NH<sub>2</sub>Cl measured by the PTR-TOF-MS, which is a much less volatile DBP. The green lines in (c) serve as the "baseline" for NCl<sub>3</sub> and CO<sub>2</sub> to aid in visualization. (b) and (d) Time-series plots of swimmer counts in the competition pool (gray bars; the left axis) and relative humidity (yellow, orange, and dark red lines; the first right axis). Relative humidity was recorded by the Lascar temperature and humidity logger (yellow line) at a height 50 cm above the pool surface and two NEMo monitors at heights of 1.2 m (orange line) and 4.7 m (dark red line) above the pool surface.

the dynamic behavior in the gas phase within the air space of an indoor pool facility, as observed in this study.

An increase in RH was observed during active periods of swimming. The dynamic behavior of RH was qualitatively similar to the behaviors of gas-phase  $\rm CO_2$  and  $\rm NCl_3$  concentrations. When the pool was under heavy use during the evening of November 21 and during both the morning and evening of November 22 and 23, the RH probe (50 cm above the pool surface) showed a mean RH of 63%, with peak values between 68 and 80%. The elevated RH can be attributed to the evaporation of water droplets and splashes induced by swimming.

Gas-phase concentrations of NCl<sub>3</sub> and CO<sub>2</sub> during the final sessions in the evening were slightly higher than during the preliminary sessions in the morning on November 22 and 23. Even though multiple factors can influence gas-phase NCl<sub>3</sub> and CO<sub>2</sub> dynamics, the energy imparted to the water by the swimmers during the final sessions may be greater than that during the preliminary sessions. This can improve liquid-to-gas transfer and result in higher gas-phase concentrations. Previous measurements in indoor swimming pools indicate that swimming performed by individual competitive swimmers can induce stronger liquid-to-gas transfer of NCl<sub>3</sub> than that induced by a child playing in the pool due to stronger mechanical mixing of the water during swimming.<sup>11</sup>

The magnitude of the CO<sub>2</sub> and NCl<sub>3</sub> concentration profiles on November 21 were lower than those on November 22 and 23. This can be due, in part, to variations in the outdoor air exchange rate (AER<sub>outdoor</sub>), which was higher on November 21. The CO<sub>2</sub> concentration decay rates obtained within 1–2 h after the preliminary or final sessions, which is used as a proxy for AER<sub>outdoor</sub>, were 18–55 and 51–85% higher on November 21 than those on November 22 and 23, respectively (Figures S6–S10).

The gas-phase NCl<sub>3</sub> concentration during closing hours (10 PM to 7 AM) was relatively low and stable, with a mean NCl<sub>3[PTR-MS]</sub> of 54 ppb in the bulk air during the nights of November 21 and 23. The gas-phase CO<sub>2</sub> concentration dropped to outdoor levels, with steady-state concentrations of 402–432 ppm. The RH was stable during the night, ranging from 55 to 60%. The NCl<sub>3[PTR-MS]</sub> presents an increasing trend from 12 PM on November 21 to 6 AM on November 22. Higher values were periodically measured during the night compared to those during active periods of swimming on November 21, potentially due to the higher AER<sub>outdoor</sub> during the daytime (CO<sub>2</sub> decay rate: 1.36 h<sup>-1</sup>, post-preliminary session) relative to the evening (CO<sub>2</sub> decay rate: 0.9 h<sup>-1</sup>, post-final session) on November 21.

Short-Term Temporal Variations in Gas-Phase NCI<sub>3</sub> Concentrations During the Swim Meet. Figure 2 shows the variation in NCl<sub>3</sub> and CO<sub>2</sub> concentrations on a shorter time scale (minutes, seconds) during the preliminary (Figure 2a,b.) and final (Figure 2c,d.) sessions on November 23, where the NCl<sub>3[PTR-MS]</sub> and CO<sub>2</sub> concentrations are presented with a time resolution of 1 s. The influence of active swimming on the NCl<sub>3</sub> concentration was observed at ~9 AM when swimmers started to warm up in the pool before the preliminary session. At this time, sudden increases in NCl<sub>3[OD-CRDS]</sub> from 23 to 78 ppb in the bulk air and 56 to 124 ppb at the pool surface were observed, corresponding to an increase in swimmer counts from 4 to 105. The concentration profile for gas-phase CO<sub>2</sub> matched that of NCl<sub>3</sub>, with peak concentrations of 746-983 ppm and 133-162 ppb for CO<sub>2</sub> and NCl<sub>3[OD-CRDS]</sub>, respectively, observed between 10:36 and 10:48 AM in the pool surface air. NCl<sub>3</sub> and CO<sub>2</sub> gradually decreased from ~11 AM to 2 PM with the decreasing number of swimmers, reaching a background level similar to the period before the preliminary session. Gas-phase NCl<sub>3</sub> and CO<sub>2</sub> concentrations exhibited strong fluctuations over the selected periods, which can be observed by the spikes in the  $NCl_{3[PTR-MS]}$  and  $CO_2$  concentration profiles. The fluctuations were more significant when there was a great number of swimmers in the pool and more obvious in the pool surface air than the bulk air, which supports the hypothesis that they are induced by active swimming.

A noteworthy dynamic feature in gas-phase NCl<sub>3</sub> and CO<sub>2</sub> concentrations is further illustrated in Figure 2c,d, where we focus on a 1 h period during the final session on November 23. Spikes in NCl<sub>3[PTR-MS]</sub> and CO<sub>2</sub> concentrations were observed in both the pool surface and bulk air, but the magnitude in the surface air is much greater. We hypothesize that active swimming induces a localized enhancement of liquid-to-gas transfer of NCl<sub>3</sub> and CO<sub>2</sub> around the swimmer, leading to higher concentrations of gas-phase NCl<sub>3</sub>, which is detected as spikes in the concentration by the PTR-TOF-MS when the swimmers approached the sampling inlet. It is also possible that the agitation of pool water by swimmers generates airborne water droplets, which undergo deposition and evaporation on the membrane filter, thereby inducing a spike in the concentration profile. We found that the gas-phase concentration of monochloramine (NH<sub>2</sub>Cl; the light blue line in Figure 2c), which is a DBP with a greater aqueous-phase concentration but a much smaller Henry's law constant, did not exhibit prominent spikes following those of NCl<sub>3</sub> and CO<sub>2</sub>. This suggests that most of the observed spikes in NCl<sub>3</sub> were not caused by the deposition and subsequent evaporation of water droplets on the filter. If droplets were evaporating on the filter, the gas-phase concentration of NH2Cl should exhibit the most prominent spikes. The negative peak observed at ~7:43 PM was likely caused by a gust of fresh air due to the opening-closing of exit doors. The peak is closely mirrored in the measured NH2Cl, NCl3, and CO2 concentrations, demonstrating that the NH2Cl measurement is not smoothed out by long adsorption/desorption processes in the sampling

We believe that the spikes in the concentration of both the gas-phase  $NCl_3$  and  $CO_2$  are mainly attributed to liquid-to-gas transfer. Surprisingly, only some of the spikes in the  $NCl_3$  concentration were mirrored by spikes in the  $CO_2$  concentration at the surface air sampling location. Conversely, all  $CO_2$  concentration spikes seemed to be mirrored by spikes in the  $NCl_3$  concentration. The reason is unclear and needs further investigation.

Correlations between Gas-Phase NCl<sub>3</sub> Concentrations with CO<sub>2</sub> and RH. Correlations between gas-phase NCl<sub>3</sub> concentrations with CO<sub>2</sub> and RH are further demonstrated in Figure 3, where NCl<sub>3[PTR-MS]</sub> and NCl<sub>3[OD-CRDS]</sub> are plotted against the CO<sub>2</sub> concentration and RH, measured by the Lascar probe (50 cm above pool surface). Only NCl<sub>3</sub> concentrations measured at the pool surface air sampling location were incorporated due to its proximity to the Lascar probe. NCl<sub>3[OD-CRDS]</sub> and NCl<sub>3[PTR-MS]</sub> correlate significantly with the pool air RH and CO<sub>2</sub> concentration, with Spearman's rank correlation coefficients (Spearman's  $\rho$ ) of 0.759 and 0.844 for RH and 0.837 and 0.854 for CO<sub>2</sub>, respectively. A similar correlation between gasphase CO<sub>2</sub> and NCl<sub>3</sub> was found in a recent study in an indoor pool in Norway, where they presented a correlation coefficient of 0.8.<sup>31</sup>

The strong correlation among RH and gas-phase CO<sub>2</sub> and NCl<sub>3</sub> concentrations in this study indicate that water vapor,

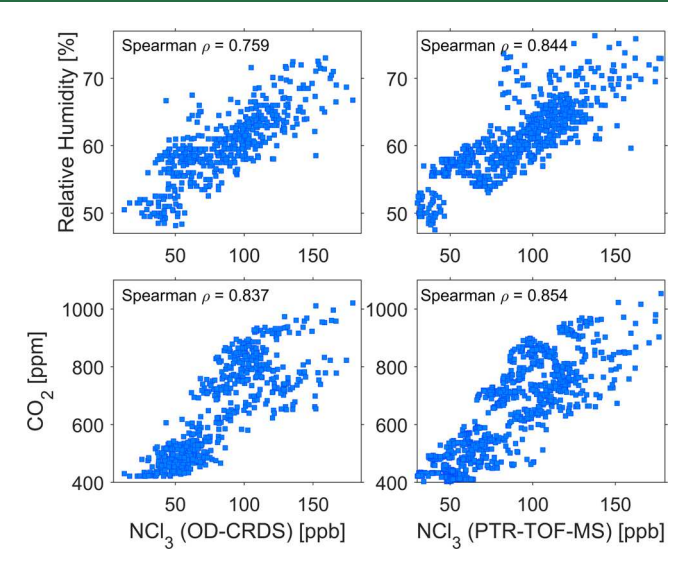


Figure 3. Correlation plots of the NCl $_3$  concentration measured by the OD-CRDS and PTR-TOF-MS at the pool surface sampling location with relative humidity (top) measured by the Lascar temperature and humidity logger at a height of 50 cm above the pool surface, and CO $_2$  concentration (bottom) at the pool surface sampling location. The NCl $_3$  concentrations from the PTR-TOF-MS are 30 s averages. Spearman's rank correlation coefficients (Spearman's  $\rho$ ) are listed.

 ${\rm CO_2}$ , and  ${\rm NCl_3}$  share similar physical transport processes in pool air. Here, we present a speculated liquid-to-air transfer scheme that can explain the significant correlations. A previous study in an indoor swimming pool indicated that the measured gas-phase  ${\rm NCl_3}$  concentration is only  ${\sim}1\%$  of the equilibrium concentration, estimated by the aqueous-phase concentration and Henry's law constant. A deviation from the equilibrium between the aqueous-phase and gas-phase concentration nearly always exists, as the pool air is constantly diluted with outdoor air. This deviation from equilibrium represents a driving force for the net transfer from the liquid to gas phase, which, in turn, results in a continuous flux of  ${\rm NCl_3}$  from the water to pool air through the water—air interface.

When swimmers are present in the pool, they may create bubbles in the water by entraining air into the water and later inducing the formation of water droplets with a size range from tens of nanometers to hundreds of micrometers, via the burst of bubbles at the air-water interface, a process similar to sea spray formation.<sup>62,63</sup> Swimming can also induce waves and water splashes. The formed waves, splashes, and water droplets may significantly increase the surface area of the water-air interface, which will increase the rate of the liquid-to-air transfer of volatile compounds. Therefore, compared to a calm and flat pool surface, active swimming will result in higher gasphase NCl<sub>3</sub> concentrations. Before the formed waves, splashes, and water droplets deposit back into the water, the CO<sub>2</sub> and water molecules are released to the air as they evaporate, leading to an increase in gas-phase CO<sub>2</sub> concentration and RH. In addition, droplets between 100 nm and 1  $\mu$ m can have a long residence time in indoor air, therefore they are likely to stay airborne until fully evaporated.<sup>64</sup> Additional measurements by aerosol instruments are needed to define the increase in the surface area of water droplets during swimming.

Spatial Variations in Gas-Phase  $NCl_3$  Concentrations within the Aquatic Center. Based on the  $NCl_{3[PTR-MS]}$  and  $NCl_{3[OD-CRDS]}$  measurements multiplexed between the surface

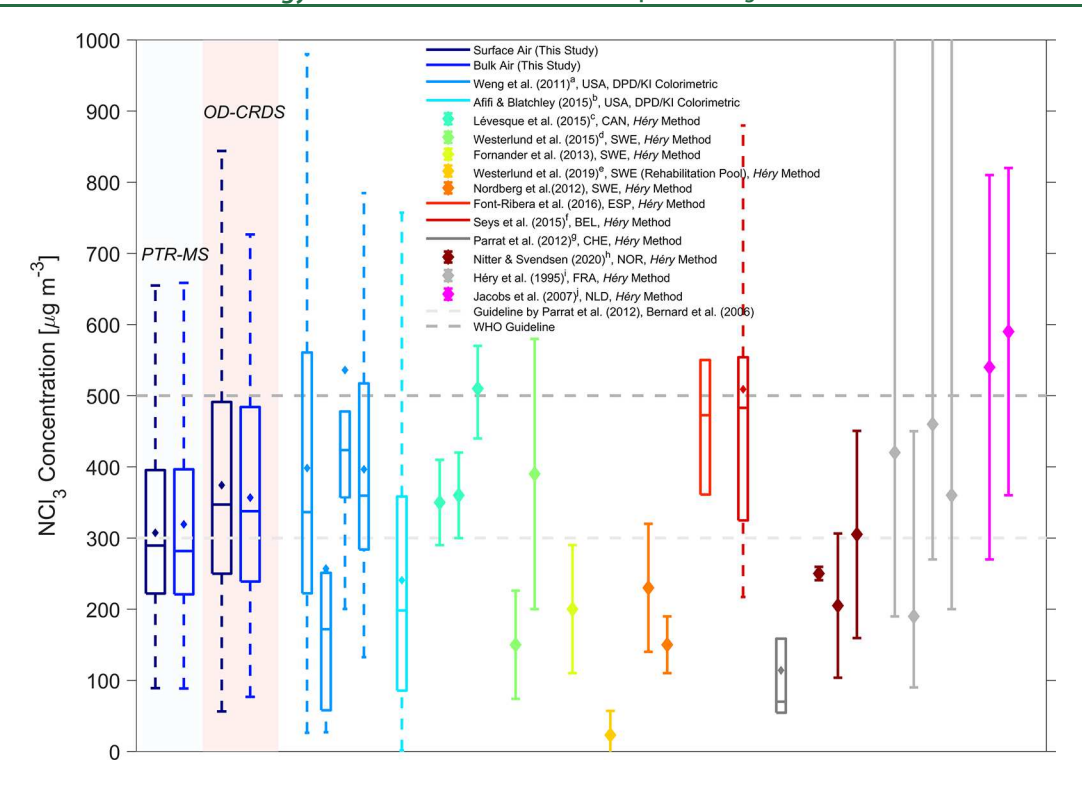


Figure 4. Comparison of the NCl<sub>3</sub> concentration measured in this study with previous studies in indoor swimming pools. Boxplots represent the interquartile range, whiskers represent the 5th and 95th percentiles, and midbars represent medians. Diamond markers represent the means and the error bars indicate the standard deviations (except for Hery et al., where the error bars represent the range of the measured concentrations, and Lévesque et al., where the error bars represent the 95% confidence interval). The pool location is listed at the country level. The measurement method is listed. The Hery Method refers to Hery et al. <sup>a</sup>Data extracted from Figures 1–4 in Weng et al., corresponding to pool A–D. Each boxplot represents the concentration measured for a pool. Replotted as a boxplot. Pool A is the same as the current study. pH of pool A = 7.5. Temperature of pool = 26 °C. Outdoor AER of pool  $C \sim 9 \text{ h}^{-1}$ . Total AER of pool  $D = 3.3-5 \text{ h}^{-1}$ . <sup>b</sup>Data extracted from Figure 6 in Afifi and Blatchley and replotted as a boxplot. Outdoor AER  $\sim 9 \text{ h}^{1}$ . pH = 7.0–8.2. Temperature = 26–28 °C. Three values correspond to the concentrations measured in the morning, afternoon, and evening in Lévesque et al. Outdoor AER = 0–4 h<sup>-1</sup>. <sup>d</sup>Concentrations measured at the exercise pool (left) and aquaerobic (right) in Westerlund et al.. Temperature = 27–37 °C. <sup>c</sup>Concentrations measured by stationary sampling in Westerlund et al. Temperature = 31–34 °C. <sup>f</sup>Data extracted from Figure 1 in Seys et al. and replotted as a boxplot. <sup>g</sup>The mean concentrations in Figure 1 in Parrat et al. were extracted and replotted as a boxplot. <sup>h</sup>Concentrations at facility 1 in the evening (left), facility 2 in the morning (middle), and facility 2 in the evening (right). Outdoor AER of facility 1 and 2 = 0.9 and 6.6 h<sup>-1</sup>. pH of facility 1 and 2 = 7.12 and 7.02. Temperature of facility 1 and 2 = 28 and 26.5 °C. Concentrations for two swimming pools (two on the left) and two recreational pools (two on the right). They represent

air and bulk air sampling locations, vertical mixing profiles in NCl<sub>3</sub> at the competition pool can be observed. The sampling locations were chosen so that they were out of the direct line of any supply air vents. The bulk air sampling location was directly above the water, while the surface air sampling location was shifted from above the water surface by about 1 m to avoid splashing water entering the sampling tube. We consider the slight horizontal shift inconsequential in this regard. No obvious difference in the gas-phase NCl<sub>3</sub> and CO<sub>2</sub> concentration was found between the pool bulk air and return air. The supply air concentrations were generally lower than the other three sampling locations.

On average, a well-mixed vertical profile was observed for NCl<sub>3</sub>; the median and mean mixing ratios measured at the pool surface air and bulk air were similar (Figure 4). During low-activity swimming periods, no vertical gradient was observed over the course of the measurement campaign. However, during the morning session on November 23 (Figure 2a), a significant vertical gradient was observed, with up to a 50% higher NCl<sub>3</sub> concentration in the surface air than in the bulk air. A vertical gradient was also observed for CO<sub>2</sub> (Figure 2a) and RH during the same period (Figure 2b). Unfortunately,

because of the high RH, the NCl<sub>3[NEMo A]</sub>, and NCl<sub>3[NEMo B]</sub> readings were unreliable during this period (see the SI).

The observed vertical NCl<sub>3</sub> gradient was inconsistent. It was not present at similar measured NCl<sub>3</sub> concentrations, e.g., during the final session on November 23 (Figure 2c.). If the sharp peaks, corresponding to droplets and splashes, are neglected, the measured NCl<sub>3[PTR-MS]</sub> evolves seamlessly over the switching events between the surface air and bulk air sampling points, as shown by the fitted baseline concentration curves in Figure 2c.

During the preliminary measurement campaign with the OD-CRDS at this site, we also sampled air just above the water surface (Figure S3). While we were not able to sample close to the water surface during periods of active swimming, we manually moved the sampling tube to right above the water level directly following a period of high activity. On several occasions, we observed significantly higher NCl<sub>3</sub> concentrations at the water level than at 1 m above the pool surface (Figure S9). Similar to the current observations, this effect was inconsistent. These observations indicate that the NCl<sub>3</sub> "bubble" suspended above the surface of the water has a transient nature in both size and prevalence at this natatorium.

Comparison of Analytical Techniques for Gas-Phase NCl<sub>3</sub> Measurement. The NCl<sub>3</sub> concentration time series (Figures 1 and 2) indicates that the corrected NCl<sub>3[PTR-MS]</sub> follows NCl<sub>3[OD-CRDS]</sub> exactly. The NEMo IAQ monitor is a more affordable instrument compared to the PTR-TOF-MS and OD-CRDS for monitoring NCl<sub>3</sub> in the air of indoor pools. The concentrations reported by the two NEMo monitors agree with those from the PTR-TOF-MS or OD-CRDS during some periods of the swim meet (e.g., from 3 to 9 PM on November 21); however, sharp decreases in NCl<sub>3[NEMo A]</sub> and NCl<sub>3[NEMo B]</sub> were observed when the RH increased close to ~65% during active swimming periods (e.g., 12 PM on November 22). It is known that the opacity signal of the iodide-infused window, which is used to determine the concentration, is influenced by RH. Specifically, opacity increases with RH. An internal RH monitor with an in-built algorithm in the software is used to automatically correct the NCl<sub>3</sub> signal for interference based on RH. However, the algorithm is not effective enough and once the instrument is exposed to high RH, and the reading becomes unreliable for several hours. From a practical perspective, the NEMo devices seem to be constrained to RH values below 65%. In addition,  $NCl_{3[NEMo\ A]}$  and  $NCl_{3[NEMo\ B]}$  were systematically lower than NCl<sub>3[PTR-MS]</sub> during the night for unknown reasons, when the RH did not exceed 65%.

Comparison with Previous NCl<sub>3</sub> Measurements in Indoor Swimming Pools. The gas-phase NCl<sub>3</sub> mixing ratios measured in this study were converted to mass concentrations and plotted as boxplots to be compared with those reported in previous studies  $^{10-13,28,31,42,67-72}$  (Figure 4). The mean mass concentrations measured by the PTR-TOF-MS and OD-CRDS in the pool surface air and bulk air range from 307 to 374  $\mu$ g m<sup>-3</sup>, with the interquartile ranges spanning from 221 to 491  $\mu$ g m<sup>-3</sup>. The mean concentrations slightly exceeded the gas-phase NCl<sub>3</sub> exposure guideline proposed by Parrat et al. and Bernard et al.  $^{9,12}$  (300  $\mu$ g m<sup>-3</sup>), while the 75th percentiles are lower than the World Health Organization (WHO) guideline (500  $\mu$ g m<sup>-3</sup>) $^{73}$  (dark and light gray lines in Figure 4)

NCl<sub>3</sub> mass concentrations reported in previous studies of chlorinated indoor pools vary across a wide range, as many factors can influence the gas-phase NCl<sub>3</sub> concentration, such as bather loading, ventilation conditions, and pool type. 10-13,28,31,42,67-72 Most studies show mean/median concentrations between 114 and 590  $\mu$ g m<sup>-3</sup>, which are within the range of the 5th and 95th percentiles of the measured concentrations in this study. Lévesque et al. 10 demonstrated a decrease in NCl3 concentrations with an increase in the outdoor AER. Weng et al.<sup>11</sup> reported a median concentration of 423  $\mu g$  m<sup>-3</sup> in a pool with a high outdoor AER of  $\sim 9 \text{ h}^{-1}$ . Relatively high concentrations under such an AER might be attributable to intense use during a high school swimming competition. Afifi and Blatchley<sup>28</sup> reported lower values in the same pool under normal use. Nitter and Svendsen<sup>31</sup> showed similar concentrations of the gas-phase NCl<sub>3</sub> in two swimming pools in Norway, while the outdoor AER of facility 2 was much higher than facility 1. The authors attributed it to the higher swimmer load and hydraulic retention time in facility 2. The pH of the pool water in the selected studies generally varied in a narrow range from ~7 to 8. The temperatures of the swimming pools were mostly between 26 and 28.5 °C. Westerlund et al. 69 reported higher temperatures between 31 and 34 °C for 10 rehabilitation pools

in Sweden. A higher temperature should result in a greater escape potential of the volatile DBPs. However, the gas-phase concentration of NCl<sub>3</sub> was only 23 ( $\pm$ 34)  $\mu$ g m<sup>-3</sup>, potentially due to the relatively small area of the pool surfaces (15–100 m<sup>2</sup>) and lack of active swimmers to agitate the pool water, as the pools are used for rehabilitation purposes.

Differences in measurement techniques can affect the comparison between studies, particularly because previous measurements are generally not selective to NCl<sub>3</sub> but provide a sum of chlorine-containing species<sup>44</sup> or all oxidizing species<sup>11</sup> in the air of swimming pools. Most of the previous studies listed in Figure 4 adopted the offline measurement method proposed by Hery et al., 44 which is based on reducing NCl<sub>3</sub> to chloride (Cl<sup>-</sup>) on a chemical filter cassette. The gas-phase NCl<sub>3</sub> concentration is determined by the volume of air being sampled and the mass of the converted Cl<sup>-</sup>, which is analyzed by ion chromatography. Another offline measurement method is to trap gas-phase NCl<sub>3</sub> in chemical solutions (N,N-diethyl-pphenylenediamine/potassium iodide) and quantify it via colorimetric measurement. 11,28 Ion mobility spectrometry can provide NCl<sub>3</sub> measurements with a high temporal resolution, which cannot be achieved by offline techniques.<sup>29</sup> However, this method is not commonly used in indoor swimming pools. In addition, the iodide-adduct chemical ionization mass spectrometer (I-CIMS) can provide online quantification of gas-phase NCl<sub>3</sub>. In a recent study, it has been employed to study the formation of NCl<sub>3</sub> in indoor air during bleach cleaning.3

## ASSOCIATED CONTENT

# Supporting Information

The Supporting Information is available free of charge at https://pubs.acs.org/doi/10.1021/acs.est.0c07413.

Calibration and operational conditions of the PTR-TOF-MS, design and operation of the portable CRDS in the OD-CRDS, gas-phase NCl<sub>3</sub> measurements with NEMo, an automated valve system for spatially resolved indoor air sampling, RH measurements, swimmer counts, implications of this study for ventilation systems in aquatic centers, and implications for inhalation exposure to NCl<sub>3</sub> and CO<sub>2</sub> among swimmers (PDF)

# AUTHOR INFORMATION

# **Corresponding Authors**

Brandon E. Boor — Lyles School of Civil Engineering, Purdue University, West Lafayette, Indiana 47907, United States; Ray W. Herrick Laboratories, Center for High Performance Buildings, Purdue University, West Lafayette, Indiana 47907, United States; orcid.org/0000-0003-1011-4100; Email: bboor@purdue.edu

Ernest R. Blatchley III — Lyles School of Civil Engineering, Purdue University, West Lafayette, Indiana 47907, United States; Division of Environmental and Ecological Engineering, Purdue University, West Lafayette, Indiana 47907, United States; orcid.org/0000-0002-4561-8635; Email: blatch@purdue.edu

#### **Authors**

Tianren Wu – Lyles School of Civil Engineering, Purdue University, West Lafayette, Indiana 47907, United States; Ray W. Herrick Laboratories, Center for High Performance

- Buildings, Purdue University, West Lafayette, Indiana 47907, United States; orcid.org/0000-0001-9214-3719
- Tomas Földes Aquality Technologies Srl, 1050 Brussels, Belgium; Spectroscopy, Quantum Chemistry, and Atmospheric Remote Sensing, Université libre de Bruxelles (ULB), 1050 Brussels, Belgium
- Lester T. Lee Lyles School of Civil Engineering, Purdue University, West Lafayette, Indiana 47907, United States
- Danielle N. Wagner Lyles School of Civil Engineering, Purdue University, West Lafayette, Indiana 47907, United States; Ray W. Herrick Laboratories, Center for High Performance Buildings, Purdue University, West Lafayette, Indiana 47907, United States
- Jinglin Jiang Lyles School of Civil Engineering, Purdue University, West Lafayette, Indiana 47907, United States; Ray W. Herrick Laboratories, Center for High Performance Buildings, Purdue University, West Lafayette, Indiana 47907, United States; ⊚ orcid.org/0000-0001-6271-0436
- Antonios Tasoglou RJ Lee Group Inc., Monroeville, Pennsylvania 15146, United States; orcid.org/0000-0001-9767-5343

Complete contact information is available at: https://pubs.acs.org/10.1021/acs.est.0c07413

#### **Notes**

The authors declare the following competing financial interest(s): Tomas Földes is a founder and shareholder of Aquality Technologies SRL, the company commercializing OD-CRDS for NCl3 measurement. The OD-CRDS for NCl3 measurement is also described in International Patent Application Number PCT/EP2019/061418, applicant: Universit libre de Bruxelles, inventor: Tomas Földes.

## ACKNOWLEDGMENTS

This work was financially supported by the National Science Foundation (CBET-1847493 to B.E.B.) and a grant from the Council for the Model Aquatic Health Code (to E.R.B. III). T.F. would like to thank the Brussels-Capital Region's Innoviris for financial support during the development of the OD-CRDS and E. Chauveheid and O. Brigode from Vivaqua Laboratory, Belgium, for conducting numerous intercomparison studies. He would also like to thank M. Cottet-Providence from Engie Lab Cylergie for the opportunity to conduct an intercomparison campaign at their experimental pool.

# **■** REFERENCES

- (1) Richardson, S. D.; DeMarini, D. M.; Kogevinas, M.; Fernandez, P.; Marco, E.; Lourencetti, C.; Ballesté, C.; Heederik, D.; Meliefste, K.; McKague, A. B.; et al. What's in the Pool? A Comprehensive Identification of Disinfection by-Products and Assessment of Mutagenicity of Chlorinated and Brominated Swimming Pool Water. *Environ. Health Perspect.* **2010**, *118*, 1523–1530.
- (2) Weaver, W. A.; Li, J.; Wen, Y.; Johnston, J.; Blatchley, M. R.; Blatchley, E. R., III Volatile Disinfection By-Product Analysis from Chlorinated Indoor Swimming Pools. *Water Res.* **2009**, *43*, 3308–3318
- (3) Parinet, J.; Tabaries, S.; Coulomb, B.; Vassalo, L.; Boudenne, J.-L. Exposure Levels to Brominated Compounds in Seawater Swimming Pools Treated with Chlorine. *Water Res.* **2012**, *46*, 828–836.
- (4) Kristensen, G. H.; Klausen, M. M.; Hansen, V. A.; Lauritsen, F. R. On-line Monitoring of the Dynamics of Trihalomethane Concentrations in a Warm Public Swimming Pool Using an Unsupervised Membrane Inlet Mass Spectrometry System with Off-

- site Real-time Surveillance. Rapid Commun. Mass Spectrom. 2010, 24, 30-34.
- (5) Manasfi, T.; Temime-Roussel, B.; Coulomb, B.; Vassalo, L.; Boudenne, J.-L. Occurrence of Brominated Disinfection Byproducts in the Air and Water of Chlorinated Seawater Swimming Pools. *Int. J. Hyg. Environ. Health* **2017**, 220, 583–590.
- (6) Tardif, R.; Catto, C.; Haddad, S.; Simard, S.; Rodriguez, M. Assessment of Air and Water Contamination by Disinfection By-Products at 41 Indoor Swimming Pools. *Environ. Res.* **2016**, *148*, 411–420.
- (7) Tsamba, L.; Correc, O.; Couzinet, A. Chlorination By-Products in Indoor Swimming Pools: Development of a Pilot Pool Unit and Impact of Operating Parameters. *Environ. Int.* **2020**, *137*, No. 105566.
- (8) Li, J.; Blatchley, E. R. Volatile Disinfection Byproduct Formation Resulting from Chlorination of Organic Nitrogen Precursors in Swimming Pools. *Environ. Sci. Technol.* **2007**, *41*, 6732–6739.
- (9) Bernard, A.; Carbonnelle, S.; de Burbure, C.; Michel, O.; Nickmilder, M. Chlorinated Pool Attendance, Atopy, and the Risk of Asthma during Childhood. *Environ. Health Perspect.* **2006**, 114, 1567–1572
- (10) Lévesque, B.; Vézina, L.; Gauvin, D.; Leroux, P. Investigation of Air Quality Problems in an Indoor Swimming Pool: A Case Study. *Ann. Occup. Hyg.* **2015**, *59*, 1085–1089.
- (11) Weng, S.; Weaver, W. A.; Zare Afifi, M.; Blatchley, T. N.; Cramer, J. S.; Chen, J.; Blatchley, E. R., III Dynamics of Gas-phase Trichloramine (NCl3) in Chlorinated, Indoor Swimming Pool Facilities. *Indoor Air* **2011**, *21*, 391–399.
- (12) Parrat, J.; Donzé, G.; Iseli, C.; Perret, D.; Tomicic, C.; Schenk, O. Assessment of Occupational and Public Exposure to Trichloramine in Swiss Indoor Swimming Pools: A Proposal for an Occupational Exposure Limit. *Ann. Occup. Hyg.* **2012**, *56*, 264–277.
- (13) Jacobs, J. H.; Spaan, S.; Van Rooy, G.; Meliefste, C.; Zaat, V. A. C.; Rooyackers, J. M.; Heederik, D. Exposure to Trichloramine and Respiratory Symptoms in Indoor Swimming Pool Workers. *Eur. Respir. J.* **2007**, *29*, 690–698.
- (14) Thoumelin, P.; Monin, F.; Armandet, D.; Julien, M. J.; Massart, B. Troubles d'irritation Respiratoire Chez Les Travailleurs Des Piscines. *Doc. pour le Médecin du Trav.* 2005, *No.* 101, 43–56.
- (15) Kaydos-Daniels, S. C.; Beach, M. J.; Shwe, T.; Magri, J.; Bixler, D. Health Effects Associated with Indoor Swimming Pools: A Suspected Toxic Chloramine Exposure. *Public Health* **2008**, *122*, 195–200.
- (16) Gagnaire, F.; Azim, S.; Bonnet, P.; Hecht, G.; Hery, M. Comparison of the Sensory Irritation Response in Mice to Chlorine and Nitrogen Trichloride. *J. Appl. Toxicol.* **1994**, *14*, 405–409.
- (17) Dang, B.; Chen, L.; Mueller, C.; Dunn, K. H.; Almaguer, D.; Roberts, J. L.; Otto, C. S. Ocular and Respiratory Symptoms among Lifeguards at a Hotel Indoor Waterpark Resort. *J. Occup. Environ. Med.* **2010**, 52, 207–213.
- (18) Thickett, K. M.; McCoach, J. S.; Gerber, J. M.; Sadhra, S.; Burge, P. S. Occupational Asthma Caused by Chloramines in Indoor Swimming-Pool Air. *Eur. Respir. J.* **2002**, *19*, 827–832.
- (19) Tafrechian, S. L'asthme Aux Chloramines Chez Le Personnel Des Piscines Mémoire pour la Capacit. médecin en santé Trav. prévention des risques Prof. Paris, Fr. Univ. R. Descartes, Fac. Médecine Paris. 2008. 5.
- (20) Afifi, M. Z. Effects of UV-Based Treatment on Water and Air Chemistry in Chlorinated Indoor Pools; Purdue University, 2015.
- (21) Afifi, M. Z.; Blatchley, E. R., III Effects of UV-Based Treatment on Volatile Disinfection Byproducts in a Chlorinated, Indoor Swimming Pool. *Water Res.* **2016**, *105*, 167–177.
- (22) De Laat, J.; Boudiaf, N.; Dossier-Berne, F. Effect of Dissolved Oxygen on the Photodecomposition of Monochloramine and Dichloramine in Aqueous Solution by UV Irradiation at 253.7 nm. *Water Res.* **2010**, *44*, 3261–3269.
- (23) Li, J.; Blatchley, E. R., Iii UV Photodegradation of Inorganic Chloramines. *Environ. Sci. Technol.* **2009**, 43, 60–65.
- (24) Soltermann, F.; Widler, T.; Canonica, S.; von Gunten, U. Photolysis of Inorganic Chloramines and Efficiency of Trichloramine

- Abatement by UV Treatment of Swimming Pool Water. Water Res. 2014, 56, 280-291.
- (25) Weng, S.; Blatchley, E. R., III Ultraviolet-Induced Effects on Chloramine and Cyanogen Chloride Formation from Chlorination of Amino Acids. *Environ. Sci. Technol.* **2013**, *47*, 4269–4276.
- (26) Weng, S. C.; Li, J.; Wood, K. V.; Kenttämaa, H. I.; Williams, P. E.; Amundson, L. M.; Blatchley, E. R., III UV-Induced Effects on Chlorination of Creatinine. *Water Res.* **2013**, 47, 4948–4956.
- (27) Seader, J. D.; Henley, E. J.; Roper, D. K. Separation Process Principles; Wiley: New York, 1998; Vol. 25.
- (28) Afifi, M. Z.; Blatchley, E. R., III Seasonal Dynamics of Water and Air Chemistry in an Indoor Chlorinated Swimming Pool. *Water Res.* **2015**, *68*, 771–783.
- (29) Zwiener, C.; Schmalz, C. Ion Mobility Spectrometry to Monitor Trichloramine in Indoor Pool Air. In *Recent Advances in Disinfection By-Products*; ACS Publications, 2015; pp 431–446.
- (30) Schmalz, C.; Frimmel, F. H.; Zwiener, C. Trichloramine in Swimming Pools—Formation and Mass Transfer. *Water Res.* **2011**, *45*, 2681–2690
- (31) Nitter, T. B.; Svendsen, K. vH. Covariation amongst Pool Management, Trichloramine Exposure and Asthma for Swimmers in Norway. *Sci. Total Environ.* **2020**, No. 138070.
- (32) Liu, S.; Li, R.; Wild, R. J.; Warneke, C.; de Gouw, J. A.; Brown, S. S.; Miller, S. L.; Luongo, J. C.; Jimenez, J. L.; Ziemann, P. J. Contribution of Human-related Sources to Indoor Volatile Organic Compounds in a University Classroom. *Indoor Air* **2016**, *26*, 925–938.
- (33) Tang, X.; Misztal, P. K.; Nazaroff, W. W.; Goldstein, A. H. Volatile Organic Compound Emissions from Humans Indoors. *Environ. Sci. Technol.* **2016**, *50*, 12686–12694.
- (34) Mattila, J. M.; Lakey, P. S. J.; Shiraiwa, M.; Wang, C.; Abbatt, J. P. D.; Arata, C.; Goldstein, A. H.; Ampollini, L.; Katz, E. F.; DeCarlo, P. F.; et al. Multiphase Chemistry Controls Inorganic Chlorinated and Nitrogenated Compounds in Indoor Air during Bleach Cleaning. *Environ. Sci. Technol.* **2020**, *54*, 1730–1739.
- (35) Pagonis, D.; Algrim, L. B.; Price, D. J.; Day, D. A.; Handschy, A. V.; Stark, H.; Miller, S. L.; de Gouw, J. A.; Jimenez, J. L.; Ziemann, P. J. Autoxidation of Limonene Emitted in a University Art Museum. *Environ. Sci. Technol. Lett.* **2019**, *6*, 520–524.
- (36) Wang, C.; Collins, D. B.; Arata, C.; Goldstein, A. H.; Mattila, J. M.; Farmer, D. K.; Ampollini, L.; DeCarlo, P. F.; Novoselac, A.; Vance, M. E.; et al. Surface Reservoirs Dominate Dynamic Gas-Surface Partitioning of Many Indoor Air Constituents. *Sci. Adv.* 2020, 6, No. eaay8973.
- (37) Farmer, D. K.; Vance, M. E.; Abbatt, J. P. D.; Abeleira, A.; Alves, M. R.; Arata, C.; Boedicker, E.; Bourne, S.; Cardoso-Saldaña, F.; Corsi, R.; et al. Overview of HOMEChem: House Observations of Microbial and Environmental Chemistry. *Environ. Sci.: Processes Impacts* **2019**, 21, 1280–1300.
- (38) Lunderberg, D.; Kristensen, K.; Tian, Y.; Arata, C.; Misztal, P. K.; Liu, Y.; Kreisberg, N. M.; Katz, E. F.; DeCarlo, P.; Patel, S.; et al. Surface Emissions Modulate Indoor SVOC Concentrations through Volatility-Dependent Partitioning. *Environ. Sci. Technol.* **2020**, *54*, 6751–6760.
- (39) Dowell, C. T.; Bray, W. C. Experiments with Nitrogen Trichloride. J. Am. Chem. Soc. 1917, 39, 896–905.
- (40) Yiin, B. S.; Margerum, D. W. Nonmetal Redox Kinetics: Reactions of Sulfite with Dichloramines and Trichloramine. *Inorg. Chem.* **1990**, *29*, 1942–1948.
- (41) Walters, W. W.; Blum, D. E.; Hastings, M. G. Selective Collection of Particulate Ammonium for Nitrogen Isotopic Characterization Using a Denuder–Filter Pack Sampling Device. *Anal. Chem.* **2019**, *91*, 7586–7594.
- (42) Hery, M.; Gerber, J. M.; Hecht, G.; Subra, I.; Possoz, C.; Aubert, S.; Dieudonne, M.; Andre, J. C. Exposure to Chloraminies in a Green Salad Processing Plant. *Ann. Occup. Hyg.* **1998**, *42*, 437–451.
- (43) INRS (Santé et sécurité au travail) MétroPol. Trichlorure d'azote et autres composés chlorés M-104. http://www.inrs.fr/publications/bdd/metropol/fiche.html?refINRS=METROPOL 104.

- (44) Hery, M.; Hecht, G.; Gerber, J. M.; Gender, J. C.; Hubert, G.; Rebuffaud, J. Exposure to Chloramines in the Atmosphere of Indoor Swimming Pools. *Ann. Occup. Hyg.* **1995**, *39*, 427–439.
- (45) Romanini, D.; Kachanov, A. A.; Stoeckel, F. Diode Laser Cavity Ring down Spectroscopy. *Chem. Phys. Lett.* **1997**, 270, 538–545.
- (46) Romanini, D.; Kachanov, A. A.; Sadeghi, N.; Stoeckel, F. CW Cavity Ring down Spectroscopy. *Chem. Phys. Lett.* **1997**, 264, 316–322
- (47) Földes, T.; Čermák, P.; Macko, M.; Veis, P.; Macko, P. Cavity Ring-down Spectroscopy of Singlet Oxygen Generated in Microwave Plasma. *Chem. Phys. Lett.* **2009**, *467*, 233–236.
- (48) Didriche, K.; Lauzin, C.; Földes, T.; de Ghellinck D'Elseghem Vaernewijck, X.; Herman, M. The FANTASIO+ Set-up to Investigate Jet-Cooled Molecules: Focus on Overtone Bands of the Acetylene Dimer. *Mol. Phys.* **2010**, *108*, 2155–2163.
- (49) Ethera Labs. Trichloramine monitor NEMo TC http://www.ethera-labs.com/en/trichloramine-monitor/.
- (50) Nguyen, T.-H.; Chevallier, E.; Garcia, J.; Nguyen, T.-D.; Laurent, A.-M.; Beaubestre, C.; Karpe, P.; Tran-Thi, T.-H. Innovative Colorimetric Sensors for the Detection of Nitrogen Trichloride at Ppb Level in Swimming Pools. *Sens. Actuators*, B **2013**, 187, 622–629.
- (51) Jordan, A.; Haidacher, S.; Hanel, G.; Hartungen, E.; Herbig, J.; Märk, L.; Schottkowsky, R.; Seehauser, H.; Sulzer, P.; Märk, T. D. An Online Ultra-High Sensitivity Proton-Transfer-Reaction Mass-Spectrometer Combined with Switchable Reagent Ion Capability (PTR+SRI–MS). Int. J. Mass Spectrom. 2009, 286, 32–38.
- (52) Pepi, F.; Ricci, A.; Rosi, M. Gas-Phase Chemistry of NH x Cly+Ions. 3. Structure, Stability, and Reactivity of Protonated Trichloramine. *J. Phys. Chem. A* **2003**, *107*, 2085–2092.
- (53) Syft Technologies Ltd. Chloramine Analysis; Using SIFT-MS, 2017.
- (54) Tromp, P.; Beuse, J.; Jacobs, J.; Kooter, I.; Fantuzzi, G.; Heederik, D. In New Insight In Airborne Levels Of Chloramines In Indoor Swimming Pools: Comparison Of Off-Line Analytical Methods With On-Site SIFT-MS., Kos Island, Greece; Swimming Pool & Spa 7th International Conference, 2017.
- (55) Bruns, E.; Slowik, J. G.; El Haddad, I.; Kilic, D.; Klein, F.; Dommen, J.; Temime-Roussel, B.; Marchand, N.; Baltensperger, U.; Prévôt, A. S. H. Characterization of Gas-Phase Organics Using Proton Transfer Reaction Time-of-Flight Mass Spectrometry: Fresh and Aged Residential Wood Combustion Emissions. *Atmos. Chem. Phys.* **2017**, 705–720.
- (56) Blatchley, E. R., III; Cheng, M. Reaction Mechanism for Chlorination of Urea. *Environ. Sci. Technol.* **2010**, 44, 8529–8534.
- (57) Sander, R. Compilation of Henry's Law Constants (Version 4.0) for Water as Solvent. *Atmos. Chem. Phys.* **2015**, *15*, 4399–4981.
- (58) Jafvert, C. T.; Valentine, R. L. Reaction Scheme for the Chlorination of Ammoniacal Water. *Environ. Sci. Technol.* **1992**, 26, 577–586
- (59) Wahman, D. G. Web-Based Applications to Simulate Drinking Water Inorganic Chloramine Chemistry. *J. Am. Water Works Assoc.* **2018**, *110*, E43–E61.
- (60) Mihelcic, J. R.; Zimmerman, J. B. Environmental Engineering: Fundamentals, Sustainability, Design; John Wiley & Sons, 2014.
- (61) Davis, M. L. Water and Wastewater Engineering: Design Principles and Practice; McGraw-Hill, 2010.
- (62) Veron, F. Ocean Spray. Annu. Rev. Fluid Mech. 2015, 47, 507-538.
- (63) de Leeuw, G.; Andreas, E. L.; Anguelova, M. D.; Fairall, C. W.; Lewis, E. R.; O'Dowd, C.; Schulz, M.; Schwartz, S. E. Production Flux of Sea Spray Aerosol. *Rev. Geophys.* **2011**, *49*, No. RG2001.
- (64) Hinds, W. C. Aerosol Technology: Properties, Behaviour, and Measurement of Airborne; John Wiley & Sons, 1982.
- (65) Baxter, R. C. Designing for IAQ in Natatoriums. ASHRAE J. 2012, 54, 24.
- (66) Rosenman, K. D.; Millerick-May, M.; Reilly, M. J.; Flattery, J.; Weinberg, J.; Harrison, R.; Lumia, M.; Stephens, A. C.; Borjan, M. Swimming Facilities and Work-Related Asthma. *J. Asthma* **2015**, *52*, 52–58.

pubs.acs.org/est

- (67) Westerlund, J.; Graff, P.; Bryngelsson, I. L.; Westberg, H.; Eriksson, K.; Löfstedt, H. Occupational Exposure to Trichloramine and Trihalomethanes in Swedish Indoor Swimming Pools: Evaluation of Personal and Stationary Monitoring. *Ann. Occup. Hyg.* **2015**, *59*, 1074–1084.
- (68) Fornander, L.; Ghafouri, B.; Lindahl, M.; Graff, P. Airway Irritation among Indoor Swimming Pool Personnel: Trichloramine Exposure, Exhaled NO and Protein Profiling of Nasal Lavage Fluids. *Int. Arch. Occup. Environ. Health* **2013**, *86*, 571–580.
- (69) Westerlund, J.; Bryngelsson, I. L.; Löfstedt, H.; Eriksson, K.; Westberg, H.; Graff, P. Occupational Exposure to Trichloramine and Trihalomethanes: Adverse Health Effects among Personnel in Habilitation and Rehabilitation Swimming Pools. *J. Occup. Environ. Hyg.* **2019**, *16*, 78–88.
- (70) Nordberg, G. F.; Lundstrom, N. G.; Forsberg, B.; Hagenbjork-Gustafsson, A.; Lagerkvist, B. J. S.; Nilsson, J.; Svensson, M.; Blomberg, A.; Nilsson, L.; Bernard, A.; Dumont, X.; Bertilsson, H.; Eriksson, K. Lung Function in Volunteers before and after Exposure to Trichloramine in Indoor Pool Environments and Asthma in a Cohort of Pool Workers. *BMJ Open* **2012**, *2*, No. e000973.
- (71) Font-Ribera, L.; Kogevinas, M.; Schmalz, C.; Zwiener, C.; Marco, E.; Grimalt, J. O.; Liu, J.; Zhang, X.; Mitch, W.; Critelli, R.; Naccarati, A.; Heederik, D.; Spithoven, J.; Arjona, L.; de Bont, J.; Gracia-Lavedan, E.; Villanueva, C. M. Environmental and Personal Determinants of the Uptake of Disinfection By-Products during Swimming. *Environ. Res.* **2016**, *149*, 206–215.
- (72) Seys, S. F.; Feyen, L.; Keirsbilck, S.; Adams, E.; Dupont, L. J.; Nemery, B. An Outbreak of Swimming-Pool Related Respiratory Symptoms: An Elusive Source of Trichloramine in a Municipal Indoor Swimming Pool. *Int. J. Hyg. Environ. Health* **2015**, *218*, 386—391.
- (73) Water, S.; Organization, W. H. Guidelines for Safe Recreational Water Environments; Swimming Pools and Similar Environments 2006; Vol. 2.